October 8, 2020

Port-Hamiltonian flexible multibody dynamics

Andrea Brugnoli

[1]ISAE-SUPAERO, Toulouse

Outline

Outline

1. Previous work on multibody systems and the pH formalism
2. PH formulation of a floating body
3. Discretization
4. Construction of multibody chain

Previous wok

Using Lie Algebra and differential forms a pH model of a flexible link has already been proposed[1]. This model can be embedded in a complex multibody system[2].

Advantages:

- Modular construction of flexible systems;
- Large deformations naturally considered.

Drawbacks:

- Implementation really does not look trivial;
- Limited to one-dimensional systems;
- Numerical analysis not feasible;
- Model reduction techniques not easily applicable.

[1] A. Macchelli, C. Melchiorri, and S. Stramigioli. "Port-Based Modeling of a Flexible Link". In: *IEEE Transactions on Robotics* 23 (2007), pp. 650 –660. DOI: 10.1109/TRO.2007.898990.

[2] A. Macchelli, C. Melchiorri, and S. Stramigioli. "Port-Based Modeling and Simulation of Mechanical Systems With Rigid and Flexible Links". In: *IEEE Transactions on Robotics* 25.5 (2009), pp. 1016–1029. DOI: 10.1109/TRO.2009.2026504.

Outline

Floating frame based approach

The floating frame approach relies on the hypothesis of small deformations: elastic motion is described w.r.t a reference that follows the large rigid motion[3].

Advantages

- The most used paradigm in multibody dynamics;
- For control applications other approaches are too complex;
- Linear model reduction techniques are applicable.

Drawbacks:

- Effect due to geometric non-linearities are not considered: not suitable for large deformations (substructuring can be employed to alleviate this).

[3] Tamer M. Wasfy and Ahmed K. Noor. "Computational strategies for flexible multibody systems". In: *Applied Mechanics Reviews* 56.6 (Nov. 2003), pp. 553–613. ISSN: 0003-6900. DOI: 10.1115/1.1590354.

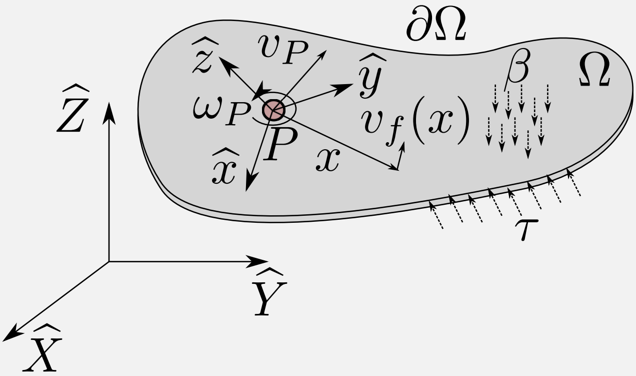

Figure: Thin floating body undergoing a surface traction $\boldsymbol{\tau}$ and body force density $\boldsymbol{\beta}$

Floating body kinematics

The velocity of a generic point is expressed by considering a small flexible displacement superimposed to the rigid motion

$$\boldsymbol{v} = \boldsymbol{v}_P + [\boldsymbol{\omega}_P]_\times (\boldsymbol{x} + \boldsymbol{u}_f) + \boldsymbol{v}_f.$$

where the cross map $[\boldsymbol{a}]_\times$ denotes the skew-symmetric matrix associated to vector $\boldsymbol{a}$. This equation is expressed in the body reference frame $\widehat{\boldsymbol{x}}, \widehat{\boldsymbol{y}}, \widehat{\boldsymbol{z}}$.

- $\boldsymbol{x}$ is the position vector of the current point;
- $\boldsymbol{v}_P$, $\boldsymbol{\omega}_P$ are the linear and angular velocities of point P;
- $\boldsymbol{v}_f := \dot{\boldsymbol{u}}_f$ the deformation velocity ;
- $m := \int_\Omega \rho \, \mathrm{d}\Omega$ the total mass;
- $\boldsymbol{s}_u := \int_\Omega \rho (\boldsymbol{x} + \boldsymbol{u}_f) \, \mathrm{d}\Omega$ the static moment;
- $\boldsymbol{J}_u := \int_\Omega \rho [\boldsymbol{x} + \boldsymbol{u}_f]_\times^\top [\boldsymbol{x} + \boldsymbol{u}_f]_\times \, \mathrm{d}\Omega$ the inertia matrix.

Canonical momenta

Consider the total energy (Hamiltonian), given by the sum of kinetic and deformation energy:

$$H = H_{\mathsf{kin}} + H_{\mathsf{def}} = \frac{1}{2}\int_\Omega \left\{\rho||\boldsymbol{v}_P + [\boldsymbol{\omega}_P]_\times(\boldsymbol{x} + \boldsymbol{u}_f) + \boldsymbol{v}_f||^2 + \boldsymbol{\Sigma} : \boldsymbol{\varepsilon}\right\} \, \mathrm{d}\Omega.$$

Canonical momenta

$$\begin{aligned}
\boldsymbol{p}_t &:= \frac{\partial H}{\partial \boldsymbol{v}_P} = m\boldsymbol{v}_P + [\boldsymbol{s}_u]_\times^\top \boldsymbol{\omega}_P + \int_\Omega \rho \boldsymbol{v}_f \, \mathrm{d}\Omega, \\
\boldsymbol{p}_r &:= \frac{\partial H}{\partial \boldsymbol{\omega}_P} = [\boldsymbol{s}_u]_\times \boldsymbol{v}_P + \boldsymbol{J}_u \boldsymbol{\omega}_P + \int_\Omega \rho[\boldsymbol{x} + \boldsymbol{u}_f]_\times \boldsymbol{v}_f \, \mathrm{d}\Omega, \\
\boldsymbol{p}_f &:= \frac{\delta H}{\delta \boldsymbol{v}_f} = \rho \boldsymbol{v}_P + \rho[\boldsymbol{x} + \boldsymbol{u}_f]_\times^\top \boldsymbol{\omega}_P + \rho \boldsymbol{v}_f, \\
\boldsymbol{\varepsilon} &:= \frac{\delta H}{\delta \boldsymbol{\Sigma}} = \boldsymbol{\mathcal{D}}^{-1}\boldsymbol{\Sigma},
\end{aligned}$$

Canonical momenta

Consider the total energy (Hamiltonian), given by the sum of kinetic and deformation energy:

$$H = H_{\text{kin}} + H_{\text{def}} = \frac{1}{2}\int_\Omega \left\{\rho||\boldsymbol{v}_P + [\boldsymbol{\omega}_P]_\times(\boldsymbol{x}+\boldsymbol{u}_f) + \boldsymbol{v}_f||^2 + \boldsymbol{\Sigma} : \boldsymbol{\varepsilon}\right\} \, \mathrm{d}\Omega.$$

Canonical momenta

$$\begin{bmatrix} \boldsymbol{p}_t \\ \boldsymbol{p}_r \\ \boldsymbol{p}_f \\ \boldsymbol{\varepsilon} \end{bmatrix} = \underbrace{\begin{bmatrix} m\boldsymbol{I}_{3\times 3} & [\boldsymbol{s}_u]_\times^\top & \mathcal{I}_\rho^\Omega & 0 \\ [\boldsymbol{s}_u]_\times & \boldsymbol{J}_u & \boldsymbol{\mathcal{I}}_{\rho x}^\Omega & 0 \\ (\mathcal{I}_\rho^\Omega)^* & (\boldsymbol{\mathcal{I}}_{\rho x}^\Omega)^* & \rho & 0 \\ 0 & 0 & 0 & \boldsymbol{\mathcal{D}}^{-1} \end{bmatrix}}_{\boldsymbol{\mathcal{M}}\text{: Mass operator}} \begin{bmatrix} \boldsymbol{v}_P \\ \boldsymbol{\omega}_P \\ \boldsymbol{v}_f \\ \boldsymbol{\Sigma} \end{bmatrix}, \qquad \begin{aligned} \mathcal{I}_\rho^\Omega &:= \int_\Omega \rho(\cdot) \, \mathrm{d}\Omega, \\ \boldsymbol{\mathcal{I}}_{\rho x}^\Omega &:= \int_\Omega \rho[\boldsymbol{x}+\boldsymbol{u}_f]_\times(\cdot). \end{aligned}$$

The mass operator $\boldsymbol{\mathcal{M}}$ is a self-adjoint, positive operator. It holds

$$H_{\text{kin}} + H_{\text{def}} = \frac{1}{2}\langle \boldsymbol{e}_{\text{kd}}, \, \boldsymbol{\mathcal{M}}\boldsymbol{e}_{\text{kd}}\rangle, \qquad \boldsymbol{e}_{\text{kd}} = [\boldsymbol{v}_P; \, \boldsymbol{\omega}_P; \, \boldsymbol{v}_f; \boldsymbol{\Sigma}]$$

Canonical momenta

Consider the total energy (Hamiltonian), given by the sum of kinetic and deformation energy:

$$H = H_{\mathrm{kin}} + H_{\mathrm{def}} = \frac{1}{2}\int_{\Omega} \left\{\rho||\boldsymbol{v}_P + [\boldsymbol{\omega}_P]_\times(\boldsymbol{x} + \boldsymbol{u}_f) + \boldsymbol{v}_f||^2 + \boldsymbol{\Sigma} : \boldsymbol{\varepsilon}\right\} \, \mathrm{d}\Omega.$$

Modified canonical momenta

$$\widehat{\boldsymbol{p}}_t := m\boldsymbol{v}_P + [\boldsymbol{s}_u]_\times^\top \boldsymbol{\omega}_P + 2\int_\Omega \rho \boldsymbol{v}_f \, \mathrm{d}\Omega, \qquad \widehat{\boldsymbol{p}}_f := \rho\boldsymbol{v}_P + \rho[\boldsymbol{x} + \boldsymbol{u}_f]_\times^\top \boldsymbol{\omega}_P + 2\rho\boldsymbol{v}_f,$$

$$\widehat{\boldsymbol{p}}_r := [\boldsymbol{s}_u]_\times \boldsymbol{v}_P + \boldsymbol{J}_u\boldsymbol{\omega}_P + 2\int_\Omega \rho[\boldsymbol{x} + \boldsymbol{u}_f]_\times \boldsymbol{v}_f \, \mathrm{d}\Omega, \qquad \boldsymbol{\mathcal{I}}_{p_f}^{\Omega} := \int_\Omega \{[\boldsymbol{p}_f]_\times + [\widehat{\boldsymbol{p}}_f]_\times\}\,(\cdot)\, \mathrm{d}\Omega,$$

Notice that the kinetic energy also depends on the flexible displacement

$$\frac{\delta H_{\mathrm{kin}}}{\delta \boldsymbol{u}_f} = [\boldsymbol{p}_f]_\times \boldsymbol{\omega}_P.$$

Equations of motion

The equations are obtained by application of the virtual work principle[4].

Linear momentum balance

$$m(\dot{\boldsymbol{v}}_P + [\boldsymbol{\omega}_P]_\times \boldsymbol{v}_P) + [\boldsymbol{s}_u]_\times^\top \dot{\boldsymbol{\omega}}_P + \int_\Omega \rho \ddot{\boldsymbol{u}}_f \, \mathrm{d}\Omega =$$
$$- [\boldsymbol{\omega}_P]_\times [\boldsymbol{\omega}_P]_\times \boldsymbol{s}_u - \int_\Omega 2\rho [\boldsymbol{\omega}_P]_\times \dot{\boldsymbol{u}}_f \, \mathrm{d}\Omega + \int_{\partial\Omega} \boldsymbol{\tau} \, \mathrm{d}\Gamma,$$

[4] Bernd Simeon. *Computational flexible multibody dynamics*. Springer, 2013, Chapter 4.

Equations of motion

The equations are obtained by application of the virtual work principle[4].

Linear momentum balance

$$
m\dot{\boldsymbol{v}}_P + [\boldsymbol{s}_u]_\times^\top \dot{\boldsymbol{\omega}}_P + \int_\Omega \rho \dot{\boldsymbol{v}}_f \, \mathrm{d}\Omega =
$$
$$
\left[m\boldsymbol{v}_P + [\boldsymbol{s}_u]_\times^\top \boldsymbol{\omega}_P + 2\int_\Omega \rho \boldsymbol{v}_f \, \mathrm{d}\Omega \right]_\times \boldsymbol{\omega}_P + \int_{\partial\Omega} \boldsymbol{\tau} \, \mathrm{d}\Gamma.
$$

[4] Bernd Simeon. *Computational flexible multibody dynamics*. Springer, 2013, Chapter 4.

Equations of motion

The equations are obtained by application of the virtual work principle[4].

Linear momentum balance

$$m\dot{\boldsymbol{v}}_P + [\boldsymbol{s}_u]_\times^\top \dot{\boldsymbol{\omega}}_P + \int_\Omega \rho \dot{\boldsymbol{v}}_f \, \mathrm{d}\Omega = [\widehat{\boldsymbol{p}}_t]_\times \boldsymbol{\omega}_P + \int_{\partial\Omega} \boldsymbol{\tau} \, \mathrm{d}\Gamma.$$

[4] Bernd Simeon. *Computational flexible multibody dynamics*. Springer, 2013, Chapter 4.

Equations of motion

The equations are obtained by application of the virtual work principle[4].

Angular momentum balance

$$
\begin{aligned}
[\boldsymbol{s}_u]_\times (\dot{\boldsymbol{v}}_P + [\boldsymbol{\omega}_P]_\times \boldsymbol{v}_P) + \boldsymbol{J}_u \dot{\boldsymbol{\omega}}_P + \int_\Omega \rho [\boldsymbol{x} + \boldsymbol{u}_f]_\times \ddot{\boldsymbol{u}}_f \, \mathrm{d}\Omega + [\boldsymbol{\omega}_P]_\times \boldsymbol{J}_u \boldsymbol{\omega}_P = \\
- \int_\Omega 2\rho [\boldsymbol{x} + \boldsymbol{u}_f]_\times [\boldsymbol{\omega}_P]_\times \dot{\boldsymbol{u}}_f \, \mathrm{d}\Omega + \int_{\partial\Omega} [\boldsymbol{x} + \boldsymbol{u}_f]_\times \boldsymbol{\tau} \, \mathrm{d}\Gamma,
\end{aligned}
$$

[4] Bernd Simeon. *Computational flexible multibody dynamics*. Springer, 2013, Chapter 4.

Equations of motion

The equations are obtained by application of the virtual work principle[4].

Angular momentum balance

$$
\begin{aligned}
[\boldsymbol{s}_u]_\times \dot{\boldsymbol{v}}_P + \boldsymbol{J}_u \dot{\boldsymbol{\omega}}_P + \int_\Omega \rho [\boldsymbol{x} + \boldsymbol{u}_f]_\times \dot{\boldsymbol{v}}_f \, \mathrm{d}\Omega = \\
\left[[\boldsymbol{s}_u]_\times^\top \boldsymbol{\omega}_P + 2 \int_\Omega \rho \boldsymbol{v}_f \, \mathrm{d}\Omega \right]_\times \boldsymbol{v}_P + \left[[\boldsymbol{s}_u]_\times \boldsymbol{v}_P + \boldsymbol{J}_u \boldsymbol{\omega}_P + 2 \int_\Omega \rho [\boldsymbol{x} + \boldsymbol{u}_f]_\times \boldsymbol{v}_f \, \mathrm{d}\Omega \right]_\times \boldsymbol{\omega}_P + \\
\int_\Omega 2 \left[\rho \boldsymbol{v}_P + \rho [\boldsymbol{x} + \boldsymbol{u}_f]_\times^\top \boldsymbol{\omega}_P \right]_\times \boldsymbol{v}_f \, \mathrm{d}\Omega + \int_{\partial\Omega} [\boldsymbol{x} + \boldsymbol{u}_f]_\times \boldsymbol{\tau} \, \mathrm{d}\Gamma.
\end{aligned}
$$

[4] Bernd Simeon. *Computational flexible multibody dynamics*. Springer, 2013, Chapter 4.

The equations are obtained by application of the virtual work principle[4].

Angular momentum balance

$$
[\boldsymbol{s}_u]_\times \dot{\boldsymbol{v}}_P + \boldsymbol{J}_u \dot{\boldsymbol{\omega}}_P + \int_\Omega \rho [\boldsymbol{x} + \boldsymbol{u}_f]_\times \dot{\boldsymbol{v}}_f \, \mathrm{d}\Omega =
$$

$$
[\widehat{\boldsymbol{p}}_t]_\times \boldsymbol{v}_P + [\widehat{\boldsymbol{p}}_r]_\times \boldsymbol{\omega}_P + \boldsymbol{\mathcal{I}}_{p_f}^\Omega \boldsymbol{v}_f + \int_{\partial\Omega} [\boldsymbol{x} + \boldsymbol{u}_f]_\times \boldsymbol{\tau} \, \mathrm{d}\Gamma.
$$

[4] Bernd Simeon. *Computational flexible multibody dynamics*. Springer, 2013, Chapter 4.

Equations of motion

The equations are obtained by application of the virtual work principle[4].

Flexibility PDE

$$\rho(\dot{\boldsymbol{v}}_P + [\boldsymbol{\omega}_P]_\times \boldsymbol{v}_P) + \rho([\dot{\boldsymbol{\omega}}_P]_\times + [\boldsymbol{\omega}_P]_\times [\boldsymbol{\omega}_P]_\times)(\boldsymbol{x} + \boldsymbol{u}_f) + \rho(2[\boldsymbol{\omega}_P]_\times \dot{\boldsymbol{u}}_f + \ddot{\boldsymbol{u}}_f) = \mathrm{Div}\,\boldsymbol{\Sigma},$$

together with boundary conditions

Neumann condition	$\boldsymbol{\Sigma} \cdot \boldsymbol{n}\vert_{\Gamma_N} = \boldsymbol{\tau}\vert_{\Gamma_N},$	$\boldsymbol{n}$ is the outward normal,
Dirichlet condition	$\boldsymbol{u}_f\vert_{\Gamma_D} = \bar{\boldsymbol{u}}_f\vert_{\Gamma_D},$	

[4] Bernd Simeon. *Computational flexible multibody dynamics*. Springer, 2013, Chapter 4.

Equations of motion

The equations are obtained by application of the virtual work principle[4].

Flexibility PDE

$$\rho \dot{\boldsymbol{v}}_P + \rho[\boldsymbol{x} + \boldsymbol{u}_f]_\times^\top \dot{\boldsymbol{\omega}}_P + \rho \dot{\boldsymbol{v}}_f = \left[\rho \boldsymbol{v}_P + \rho[\boldsymbol{x} + \boldsymbol{u}_f]_\times^\top \boldsymbol{\omega}_P + 2\rho \boldsymbol{v}_f\right]_\times \boldsymbol{\omega}_P + \mathrm{Div}\, \boldsymbol{\Sigma}.$$

together with boundary conditions

Neumann condition $\quad \boldsymbol{\Sigma} \cdot \boldsymbol{n}|_{\Gamma_N} = \boldsymbol{\tau}|_{\Gamma_N}, \quad \boldsymbol{n}$ is the outward normal,

Dirichlet condition $\quad \boldsymbol{u}_f|_{\Gamma_D} = \bar{\boldsymbol{u}}_f|_{\Gamma_D},$

[4] Bernd Simeon. *Computational flexible multibody dynamics*. Springer, 2013, Chapter 4.

Equations of motion

The equations are obtained by application of the virtual work principle[4].

Flexibility PDE

$$\rho \dot{\boldsymbol{v}}_P + \rho [\boldsymbol{x} + \boldsymbol{u}_f]_\times^\top \dot{\boldsymbol{\omega}}_P + \rho \dot{\boldsymbol{v}}_f = -\delta_{\boldsymbol{u}_f} H - \boldsymbol{\mathcal{I}}_{p_f}^* \boldsymbol{\omega}_P + \mathrm{Div}\, \boldsymbol{\Sigma}.$$

together with boundary conditions

Neumann condition	$\boldsymbol{\Sigma} \cdot \boldsymbol{n}\vert_{\Gamma_N} = \boldsymbol{\tau}\vert_{\Gamma_N},$	$\boldsymbol{n}$ is the outward normal,
Dirichlet condition	$\boldsymbol{u}_f\vert_{\Gamma_D} = \bar{\boldsymbol{u}}_f\vert_{\Gamma_D},$	

[4] Bernd Simeon. *Computational flexible multibody dynamics*. Springer, 2013, Chapter 4.

Generalized coordinates

Generalized coordinates are required for a complete formulation:

- ${}^{i}\boldsymbol{r}_P$ the position of point P in the inertial frame of reference;
- $\boldsymbol{R}$ the direction cosine matrix (other attitude parametrizations are possible);
- $\boldsymbol{u}_f$ the flexible displacement;

The direction cosine matrix is converted into a vector by concatenating its rows

$$\boldsymbol{R}_{\mathsf{v}} = \mathrm{vec}(\boldsymbol{R}^\top) = [\boldsymbol{R}_1 \ \boldsymbol{R}_2 \ \boldsymbol{R}_3]^\top,$$

where $\boldsymbol{R}_1, \boldsymbol{R}_2, \boldsymbol{R}_3$ are the rows of matrix $\boldsymbol{R}$. Furthermore the corresponding cross map will be given by

$$[\boldsymbol{R}_{\mathsf{v}}]_\times = \begin{bmatrix} [\boldsymbol{R}_1]_\times \\ [\boldsymbol{R}_2]_\times \\ [\boldsymbol{R}_3]_\times \end{bmatrix}, \qquad [\boldsymbol{R}_{\mathsf{v}}]_\times : \mathbb{R}^9 \rightarrow \mathbb{R}^{9\times 3}.$$

The overall port-Hamiltonian formulation (without including the boundary traction $\boldsymbol{\tau}$)

$$
\underbrace{\left[\begin{array}{c:c} \boldsymbol{I} & 0 \\ \hdashline 0 & \boldsymbol{\mathcal{M}} \end{array}\right]}_{\boldsymbol{\mathcal{E}}} \frac{\partial}{\partial t} \underbrace{\begin{bmatrix} {}^{i}\boldsymbol{r}_P \\ \boldsymbol{R}_{\mathsf{v}} \\ \boldsymbol{u}_f \\ \hdashline \boldsymbol{v}_P \\ \boldsymbol{\omega}_P \\ \boldsymbol{v}_f \\ \boldsymbol{\Sigma} \end{bmatrix}}_{\boldsymbol{e}} = \underbrace{\left[\begin{array}{ccc:cccc} 0 & 0 & 0 & \boldsymbol{R} & 0 & 0 & 0 \\ 0 & 0 & 0 & 0 & [\boldsymbol{R}_{\mathsf{v}}]_\times & 0 & 0 \\ 0 & 0 & 0 & 0 & 0 & \boldsymbol{I}_{3\times 3} & 0 \\ \hdashline -\boldsymbol{R}^\top & 0 & 0 & 0 & [\widehat{\boldsymbol{p}}_t]_\times & 0 & 0 \\ 0 & -[\boldsymbol{R}_{\mathsf{v}}]_\times^\top & 0 & [\widehat{\boldsymbol{p}}_t]_\times & [\widehat{\boldsymbol{p}}_r]_\times & \boldsymbol{\mathcal{I}}_{p_f}^{\Omega} & 0 \\ 0 & 0 & -\boldsymbol{I}_{3\times 3} & 0 & -(\boldsymbol{\mathcal{I}}_{p_f}^{\Omega})^* & 0 & \mathrm{Div} \\ 0 & 0 & 0 & 0 & 0 & \mathrm{Grad} & 0 \end{array}\right]}_{\boldsymbol{\mathcal{J}}} \underbrace{\begin{bmatrix} \partial_{\boldsymbol{r}_P} H \\ \partial_{\boldsymbol{R}_{\mathsf{v}}} H \\ \delta_{\boldsymbol{u}_f} H \\ \hdashline \boldsymbol{v}_P \\ \boldsymbol{\omega}_P \\ \boldsymbol{v}_f \\ \boldsymbol{\Sigma} \end{bmatrix}}_{\boldsymbol{z}}.
$$

Final pHDAE system

This system fits into the framework detailed in[5] and extends it.

$$\begin{aligned}
\boldsymbol{\mathcal{E}}(\boldsymbol{e})\partial_t \boldsymbol{e} &= \boldsymbol{\mathcal{J}}(\boldsymbol{e})\boldsymbol{z}(\boldsymbol{e}) + \boldsymbol{\mathcal{B}}_r(\boldsymbol{e})\boldsymbol{u}_\partial, \\
\boldsymbol{y}_r &= \boldsymbol{\mathcal{B}}_r^*(\boldsymbol{e})\boldsymbol{z}(\boldsymbol{e}), \\
\boldsymbol{u}_\partial &= \boldsymbol{\mathcal{B}}_\partial \boldsymbol{z}(\boldsymbol{e}) = \boldsymbol{\Sigma}\cdot\boldsymbol{n}|_{\partial\Omega} = \boldsymbol{\tau}|_{\partial\Omega}, \\
\boldsymbol{y}_\partial &= \boldsymbol{\mathcal{C}}_\partial \boldsymbol{z}(\boldsymbol{e}) = \boldsymbol{v}_f|_{\partial\Omega},
\end{aligned}$$

with $\boldsymbol{y}_r = (\boldsymbol{v}_P + [\boldsymbol{x} + \boldsymbol{u}_f]_\times^\top \boldsymbol{\omega}_P)|_{\partial\Omega}$.

Operator $\boldsymbol{\mathcal{E}}$ is positive self-adjoint, $\boldsymbol{\mathcal{J}}$ is formally skew-symmetric. The Hamiltonian satisfies

$$\partial_{\boldsymbol{e}} H = \boldsymbol{\mathcal{E}}^* \boldsymbol{z}.$$

[5] Volker Mehrmann and Riccardo Morandin. "Structure-preserving discretization for port-Hamiltonian descriptor systems". In: *Proceedings of the 59th IEEE Conference on Decision and Control*. 2019, pp. 6663–6868.

Power balance

The power balance equals the power due to the surface traction

$$
\begin{aligned}
\dot{H}(\boldsymbol{e}) &= \langle \partial_{\boldsymbol{e}} H, \partial_t \boldsymbol{e} \rangle_X, \\
&= \langle \boldsymbol{z}, \boldsymbol{\mathcal{E}} \partial_t \boldsymbol{e} \rangle_X, \quad \text{Adjoint definition}, \\
&= \langle \boldsymbol{y}_\partial, \boldsymbol{u}_\partial \rangle_{\partial\Omega} + \langle \boldsymbol{\mathcal{B}}_r^* \boldsymbol{z}, \boldsymbol{u}_\partial \rangle_{\partial\Omega}, \quad \text{I.B.P. on } \boldsymbol{\mathcal{J}}, \\
&= \int_{\partial\Omega} \boldsymbol{u}_\partial \cdot (\boldsymbol{y}_\partial + \boldsymbol{y}_r) \; \mathrm{d}\Omega, \\
&= \int_{\partial\Omega} \boldsymbol{\tau} \cdot \boldsymbol{v} \; \mathrm{d}\Gamma,
\end{aligned}
$$

where $\boldsymbol{y}_\partial + \boldsymbol{y}_r := (\boldsymbol{v}_P + [\boldsymbol{\omega}_P]_\times (\boldsymbol{x} + \boldsymbol{u}_f) + \boldsymbol{v}_f)|_{\partial\Omega} = \boldsymbol{v}|_{\partial\Omega}$ is the velocity field at the boundary.

- Generic linear elastic model can be included.
- Conservative forces are easily accounted for by introducing an appropriate potential energy. The gravitational potential

$$H_{\text{pot}} = \int_\Omega \rho g \, {}^i r_z \, \mathrm{d}\Omega = \int_\Omega \rho g \left[{}^i r_{P,z} + \boldsymbol{R}_z(\boldsymbol{x} + \boldsymbol{u}_f) \right] \, \mathrm{d}\Omega.$$

- Geometric stiffening could be considered by adding a potential energy associated to centrifugal forces or using a substructuring technique.
- If case of vanishing deformations $\boldsymbol{u}_f \equiv 0$, the Newton-Euler equations on the Euclidean group $SE(3)$ are retrieved

$$\frac{d}{dt}\begin{pmatrix} {}^i\boldsymbol{r}_P \\ \boldsymbol{R}_{\text{v}} \\ \boldsymbol{p}_t \\ \boldsymbol{p}_r \end{pmatrix} = \begin{bmatrix} 0 & 0 & \boldsymbol{R} & 0 \\ 0 & 0 & 0 & [\boldsymbol{R}_{\text{v}}]_\times \\ -\boldsymbol{R}^\top & 0 & 0 & [\boldsymbol{p}_t]_\times \\ 0 & -[\boldsymbol{R}_{\text{v}}]_\times^\top & [\boldsymbol{p}_t]_\times & [\boldsymbol{p}_r]_\times \end{bmatrix} \begin{bmatrix} \partial_{\boldsymbol{r}_P} H \\ \partial_{\boldsymbol{R}_{\text{v}}} H \\ \partial_{\boldsymbol{p}_t} H \\ \partial_{\boldsymbol{p}_r} H \end{bmatrix}.$$

Outline

Discretized system

Same procedure as always but the integration by parts is applied to the Div operator to highlight the Neumann condition.

Finite-dimensional pHDAE system

After integration by parts of the Div operator

$$\begin{aligned}\mathbf{E}(\mathbf{e})\dot{\mathbf{e}} = \mathbf{J}(\mathbf{e})\mathbf{z}(\mathbf{e}) + \mathbf{B}_d(\mathbf{e})\mathbf{u}_d + \mathbf{B}_\partial(\mathbf{e})\mathbf{u}_\partial,\\ \mathbf{y}_d := \mathbf{M}_d\widetilde{\mathbf{y}}_d = \mathbf{B}_d^\top \mathbf{z}(\mathbf{e}),\\ \mathbf{y}_\partial := \mathbf{M}_\partial\widetilde{\mathbf{y}}_\partial = \mathbf{B}_\partial^\top \mathbf{z}(\mathbf{e}).\end{aligned}$$

Dirichlet conditions

The set Γ_D for the Dirichlet condition has to be non empty, otherwise the deformation field is allowed for rigid movement, leading to a singular mass matrix. Test and state shape functions must verify an homogeneous Dirichlet condition[6].

[6] O.P. Agrawal and A.A. Shabana. "Application of deformable-body mean axis to flexible multibody system dynamics". In: *Computer Methods in Applied Mechanics and Engineering* 56.2 (1986), pp. 217–245.

Computation of the effort functions

The computation of vector $\mathbf{z}$ is based on the discrete Hamiltonian gradient:

$$\frac{\partial H_d}{\partial \mathbf{e}} = \mathbf{E}^\top \mathbf{z}, \qquad H_d = H_{d,\mathsf{kin}} + H_{d,\mathsf{def}} + H_{d,\mathsf{pot}}.$$

The only term that requires additional care is $\boldsymbol{z}_u = \delta_{\boldsymbol{u}_f} H$.
Flexible displacement contribution to the power balance

$$\dot{H}_u = \int_\Omega \frac{\partial \boldsymbol{u}_f}{\partial t} \cdot \boldsymbol{z}_u \, \mathrm{d}\Omega = \int_\Omega \frac{\partial \boldsymbol{u}_f}{\partial t} \cdot \frac{\delta H}{\delta \boldsymbol{u}_f} \, \mathrm{d}\Omega$$

Given that $\boldsymbol{u}_f = \boldsymbol{\phi}_u^\top \mathbf{u}_f, \ \boldsymbol{z}_u = \boldsymbol{\phi}_u^\top \mathbf{z}_u$, the discrete Hamiltonian rate assumes the expressions

$$\dot{H}_{u,d}(\mathbf{u}_f) = \begin{cases} \dot{\mathbf{u}}_f^\top \mathbf{M}_u \, \mathbf{z}_u, \\ \dot{\mathbf{u}}_f^\top \dfrac{\partial H_d}{\partial \mathbf{u}_f}, \end{cases} \quad \Longrightarrow \quad \mathbf{z}_u = \mathbf{M}_u^{-1} \frac{\partial H_d}{\partial \mathbf{u}_f}, \quad \text{where } \mathbf{M}_u = \int_\Omega \boldsymbol{\phi}_u \, \boldsymbol{\phi}_u^\top \, \mathrm{d}\Omega$$

Outline

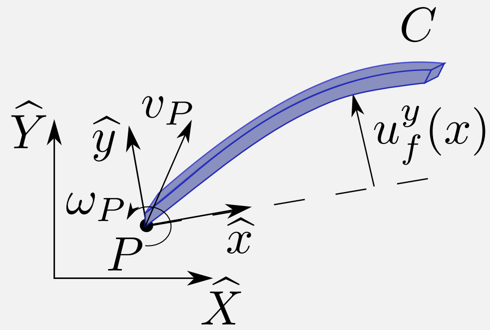

Figure: Floating beam.

Beam discretized system

Neglecting the dependence on the deformation field in the mass matrix ($\mathbf{M} =$ const)

$$\mathbf{E}\dot{\mathbf{e}} = \mathbf{J}(\mathbf{e})\mathbf{z}(\mathbf{e}) + \mathbf{B}\mathbf{u},$$
$$\mathbf{y} = \mathbf{B}^\top \mathbf{z},$$

with boundary variables

$$\mathbf{u} = [F_P^x,\ F_P^y,\ T_P^z,\ F_C^x,\ F_C^y,\ T_C^z]^\top,$$
$$\mathbf{y} = [v_P^x,\ v_P^y,\ \omega_P^z,\ v_C^x,\ v_C^y,\ \omega_C^z]^\top.$$

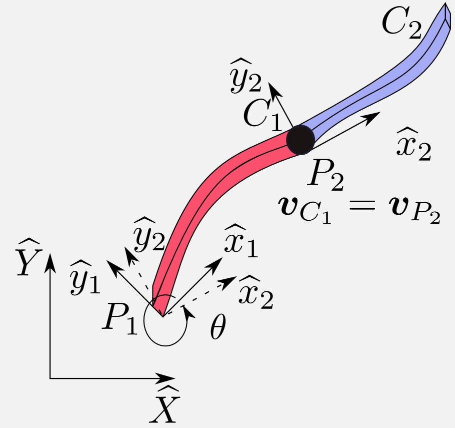

Figure: Two hinged beams.

The interconnection variables are

$$
\begin{aligned}
\mathbf{u}_1^{\text{int}} &= [F_{C_1}^x, \; F_{C_1}^y]^\top := \mathbf{F}_{C_1}, \\
\mathbf{u}_2^{\text{int}} &= [F_{P_2}^x, \; F_{P_2}^y]^\top := \mathbf{F}_{P_2}, \\
\mathbf{y}_1^{\text{int}} &= [v_{C_1}^x, \; v_{C_1}^y]^\top := \mathbf{v}_{C_1}, \\
\mathbf{y}_2^{\text{int}} &= [v_{P_2}^x, \; v_{P_2}^y]^\top := \mathbf{v}_{P_2}.
\end{aligned}
$$

Final system

Hinged interconnected beams

The transformer interconnection

$$\mathbf{u}_1^{\text{int}} = -\mathbf{R}(\theta)\mathbf{u}_2^{\text{int}}, \qquad \mathbf{y}_2^{\text{int}} = \mathbf{R}(\theta)^\top \mathbf{y}_1^{\text{int}},$$

where $\mathbf{R}(\theta)$ is the relative rotation matrix, imposes the constraints on the velocity level and gives rise to a quasi-linear index 2 pHDAE.

$$\begin{bmatrix} \mathbf{E}_1 & 0 & 0 \\ 0 & \mathbf{E}_2 & 0 \\ 0 & 0 & 0 \end{bmatrix} \begin{bmatrix} \dot{\mathbf{e}}_1 \\ \dot{\mathbf{e}}_2 \\ \dot{\boldsymbol{\lambda}} \end{bmatrix} = \begin{bmatrix} \mathbf{J}_1(\mathbf{e}_1) & 0 & -\mathbf{B}_1^{\text{int}}\mathbf{R} \\ 0 & \mathbf{J}_2(\mathbf{e}_2) & \mathbf{B}_2^{\text{int}} \\ \mathbf{R}^\top \mathbf{B}_1^{\text{int}\top} & -\mathbf{B}_2^{\text{int}\top} & 0 \end{bmatrix} \begin{bmatrix} \mathbf{z}_1 \\ \mathbf{z}_2 \\ \boldsymbol{\lambda} \end{bmatrix} + \begin{bmatrix} \mathbf{B}_{\partial 1}^{\text{ext}} & 0 \\ 0 & \mathbf{B}_{\partial 2}^{\text{ext}} \\ 0 & 0 \end{bmatrix} \begin{bmatrix} \mathbf{u}_1^{\text{ext}} \\ \mathbf{u}_2^{\text{ext}} \end{bmatrix},$$

$$\begin{bmatrix} \mathbf{y}_1^{\text{ext}} \\ \mathbf{y}_2^{\text{ext}} \end{bmatrix} = \begin{bmatrix} \mathbf{B}_{\partial 1}^{\text{ext}\top} & 0 & 0 \\ 0 & \mathbf{B}_{\partial 2}^{\text{ext}\top} & 0 \end{bmatrix} \begin{bmatrix} \mathbf{z}_1 \\ \mathbf{z}_2 \\ \boldsymbol{\lambda} \end{bmatrix}.$$

Equivalence of gyrator and transformer interconnection

The same result can be obtained by using a pHDAE system and a gyrator interconnection. It is sufficient to interchange the role of output and input of the second system $\mathbf{u}_2^{\text{int}} \leftrightarrow \mathbf{y}_2^{\text{int}}$.

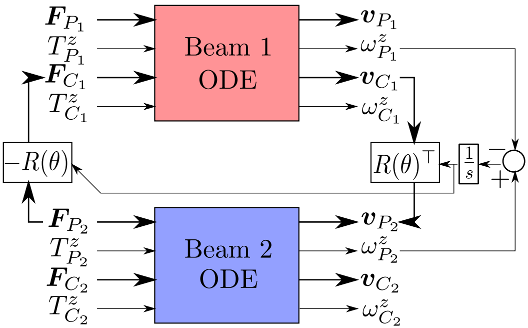

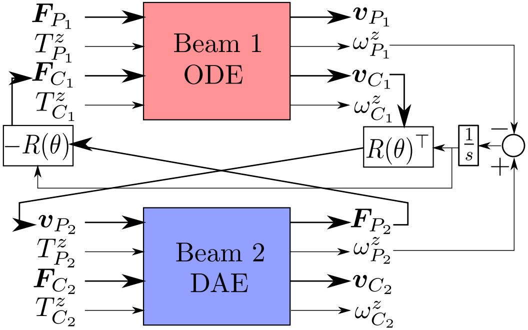

Outline

Hypothesis:

1. small angular velocities;
2. small relative configuration.

$$\begin{bmatrix} \mathbf{M}_{rr} & \mathbf{M}_{rf} & 0 \\ \mathbf{M}_{fr} & \mathbf{M}_{ff} & 0 \\ 0 & 0 & 0 \end{bmatrix} \begin{bmatrix} \dot{\mathbf{p}}_r \\ \dot{\mathbf{p}}_f \\ \dot{\boldsymbol{\lambda}} \end{bmatrix} = \begin{bmatrix} 0 & 0 & \mathbf{G}_r^\top \\ 0 & \mathbf{J}_{ff} & \mathbf{G}_f^\top \\ -\mathbf{G}_r & -\mathbf{G}_f & 0 \end{bmatrix} \begin{bmatrix} \mathbf{p}_r \\ \mathbf{p}_f \\ \boldsymbol{\lambda} \end{bmatrix} + \begin{bmatrix} \mathbf{B}_r \\ \mathbf{B}_f \\ 0 \end{bmatrix} \mathbf{u}.$$

with Hamiltonian $H = \frac{1}{2}\mathbf{p}^\top \mathbf{M} \mathbf{p}$. The modular construction of complex multi-body systems is then analogous to a sub-structuring technique[7].

[7] D. De Klerk, D. J. Rixen, and S. N. Voormeeren. "General Framework for Dynamic Substructuring: History, Review and Classification of Techniques". In: *AIAA Journal* 46.5 (2008), pp. 1169–1181. DOI: 10.2514/1.33274. URL: https://doi.org/10.2514/1.33274.

Model and index reduction

Model reduction

Such system can be reduced using Linear model reduction methods directly in the DAE[8]. Vector $\mathbf{p}_f$ is projected on a meaningful subspace $\mathbf{p}_f \approx \mathbf{V}_f^{\text{red}} \mathbf{p}_f^{\text{red}}$

$$
\begin{bmatrix} \mathbf{M}_{rr} & \mathbf{M}_{rf}^{\text{red}} & 0 \\ \mathbf{M}_{fr}^{\text{red}} & \mathbf{M}_{ff}^{\text{red}} & 0 \\ 0 & 0 & 0 \end{bmatrix} \begin{bmatrix} \dot{\mathbf{p}}_r \\ \dot{\mathbf{p}}_f^{\text{red}} \\ \dot{\lambda} \end{bmatrix} = \begin{bmatrix} 0 & 0 & \mathbf{G}_r^\top \\ 0 & \mathbf{J}_{ff}^{\text{red}} & \mathbf{G}_f^{\text{red}\top} \\ -\mathbf{G}_r & -\mathbf{G}_f^{\text{red}} & 0 \end{bmatrix} \begin{bmatrix} \mathbf{p}_r \\ \mathbf{p}_f^{\text{red}} \\ \lambda \end{bmatrix} + \begin{bmatrix} \mathbf{B}_r \\ \mathbf{B}_f^{\text{red}} \\ 0 \end{bmatrix} \mathbf{u},
$$

[8] H. Egger et al. "On Structure-Preserving Model Reduction for Damped Wave Propagation in Transport Networks". In: *SIAM Journal on Scientific Computing* 40.1 (2018), A331–A365. DOI: 10.1137/17M1125303.

Index reduction

$$\begin{aligned} \mathbf{M}\dot{\mathbf{p}} &= \mathbf{J}\mathbf{p} + \mathbf{G}^\top \boldsymbol{\lambda} + \mathbf{B}\mathbf{u}, \\ \mathbf{0} &= \mathbf{G}\mathbf{p}, \end{aligned}$$

A null space matrix can employed to eliminate the Lagrange multiplier and preserve the port-Hamiltonian structure.

$$\mathrm{range}\{\mathbf{P}\} = \mathrm{null}\{\mathbf{G}\}.$$

Then, the range of $\mathbf{P}$ automatically satisfies the constraints. Considering the transformation $\widehat{\mathbf{p}} = \mathbf{P}\mathbf{p}$ and pre-multiplying the system by $\mathbf{P}^\top$ an equivalent ODE is obtained

$$\widehat{\mathbf{M}}\ \dot{\widehat{\mathbf{p}}} = \widehat{\mathbf{J}}\ \widehat{\mathbf{p}} + \widehat{\mathbf{B}}\ \mathbf{u},$$

with $\widehat{\mathbf{M}} = \mathbf{P}^\top \mathbf{M}\mathbf{P}$, $\widehat{\mathbf{J}} = \mathbf{P}^\top \mathbf{J}\mathbf{P}$, $\widehat{\mathbf{B}} = \mathbf{P}^\top \mathbf{B}$.

Outline

Rigid rod welded to a cantilever plate

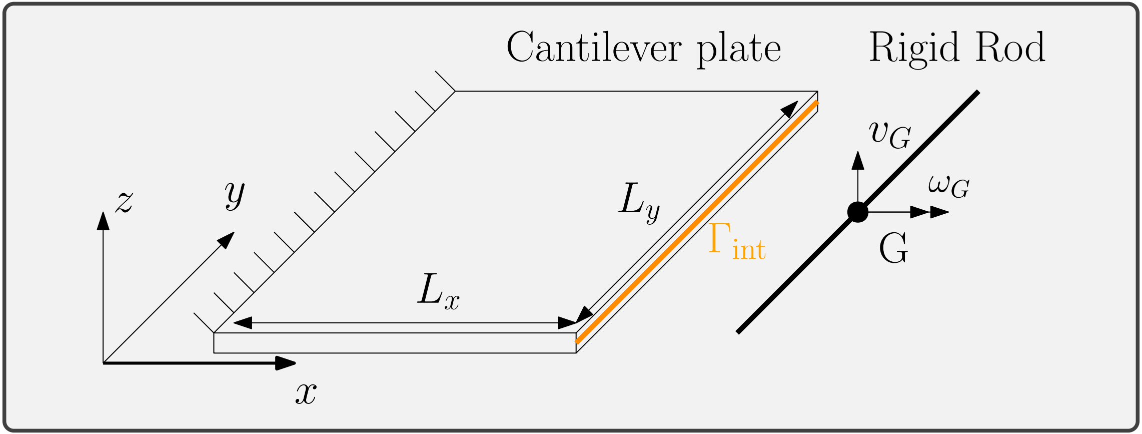

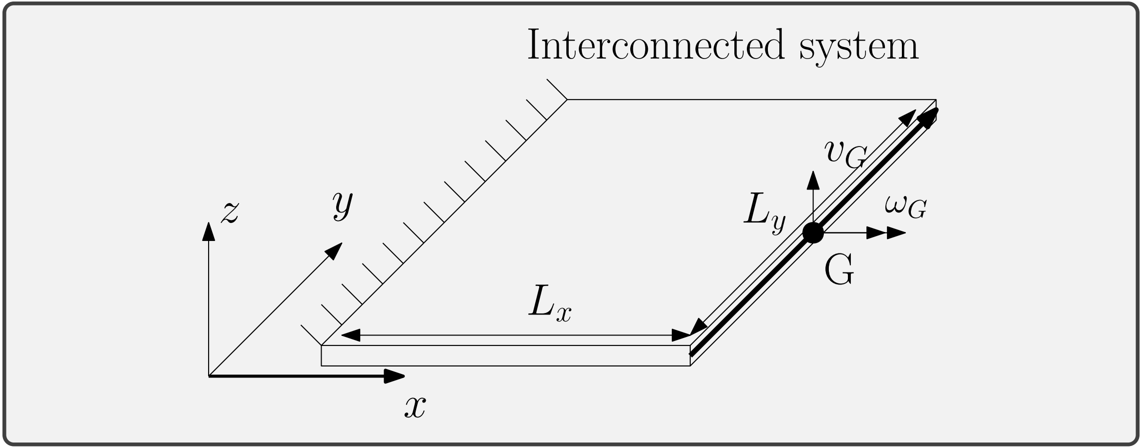
Interconnected system
v_G
L_y
ω_G
G
z
y
L_x
x

The system is composed by a cantilever plate (distributed pH) connected to a rigid rod:

$$\text{dpH} \qquad \begin{aligned} \partial_t \boldsymbol{x}_1 &= \mathcal{J}\, \delta_{\boldsymbol{x}_1} H_1, \\ \boldsymbol{u}_{\partial,1} &= \mathcal{B}_\partial\, \delta_{\boldsymbol{x}_1} H_1, \\ \boldsymbol{y}_{\partial,1} &= \mathcal{C}_\partial\, \delta_{\boldsymbol{x}_1} H_1, \end{aligned} \qquad\qquad \text{pH} \qquad \begin{aligned} \dot{\mathbf{x}}_2 &= \mathbf{J}\nabla_{\mathbf{x}_2} H_2 + \mathbf{B}\mathbf{u}_2, \\ \mathbf{y}_2 &= \mathbf{B}^\top \nabla_{\mathbf{x}_2} H_2, \end{aligned}$$

where $\mathbf{x} \in \mathbb{R}^n, \mathbf{u}_2, \mathbf{y}_2 \in \mathbb{R}^m$ and $\boldsymbol{x}_1 \in X$, $\boldsymbol{u}_{\partial,1} \in U$, $\boldsymbol{y}_{\partial,1} \in Y = U'$ belong to and Hilbert spaces and $\mathcal{B}_\partial : X \to U$, $\mathcal{C}_\partial : X \to Y$ are boundary operators.
The duality pairings for the boundary ports are denoted by

$$\langle \boldsymbol{u}_{\partial,1},\, \boldsymbol{y}_{\partial,1} \rangle_{U \times Y}\,, \qquad \langle \mathbf{u}_2,\, \mathbf{y}_2 \rangle_{\mathbb{R}^m}\,.$$

For the interconnection, consider the compact operator $\mathcal{W} : Y \to \mathbb{R}^m$ and the following power-preserving interconnection

$$\mathbf{u}_2 = -\mathcal{W}\, \boldsymbol{y}_{\partial,1}, \qquad \boldsymbol{u}_{\partial,1} = \mathcal{W}^*\, \mathbf{y}_2.$$

Boundary interconnection

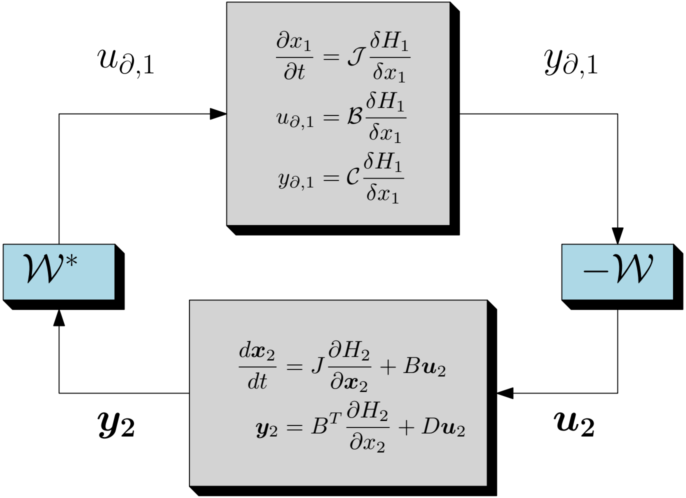

Kirchhoff plate welded to a rigid rod

Plate $(\Omega = [0, L_x] \times [0, L_y])$

$$
\begin{bmatrix} \rho h & 0 \\ 0 & \mathcal{C}_b \end{bmatrix} \frac{\partial}{\partial t} \begin{bmatrix} e_w \\ \boldsymbol{E}_\kappa \end{bmatrix} = \begin{bmatrix} 0 & -\operatorname{div}\operatorname{Div} \\ \nabla^2 & 0 \end{bmatrix} \begin{bmatrix} e_w \\ \boldsymbol{E}_\kappa \end{bmatrix}
$$

$$
\begin{aligned}
u_{\partial,\mathrm{pl}} &= e_w(x = L_x, y), \\
y_{\partial,\mathrm{pl}} &= \widetilde{q}_n(x = L_x, y).
\end{aligned}
$$

Rigid rod

$$
\begin{bmatrix} M & 0 \\ 0 & J_G \end{bmatrix} \frac{d}{dt} \begin{pmatrix} v_G \\ \omega_G \end{pmatrix} = \begin{pmatrix} F_z \\ T_x \end{pmatrix} = \boldsymbol{u}_{\mathrm{rod}},
$$

$$
\boldsymbol{y}_{\mathrm{rod}} = \begin{pmatrix} v_G \\ \omega_G \end{pmatrix},
$$

Space Y is the space of square-integrable functions with support on $\Gamma_{\mathrm{int}} = \{x = L_x\}$.
The interconnection operator provides the total force and torque acting on the rigid rod

$$
\mathcal{W} y_{\partial,\mathrm{pl}} = -\begin{pmatrix} F_z \\ T_x \end{pmatrix} = \begin{pmatrix} \int_{\Gamma_{\mathrm{int}}} y_{\partial,\mathrm{pl}} \, \mathrm{d}s \\ \int_{\Gamma_{\mathrm{int}}} (y - L_y/2) \, y_{\partial,\mathrm{pl}} \, \mathrm{d}s \end{pmatrix}.
$$

The adjoint operator provides a rigid movement as the plate input at Γ_{int}

$$
\begin{aligned}
\langle \mathcal{W} y_{\partial,\mathrm{pl}}, \, \boldsymbol{y}_{\mathrm{rod}} \rangle_{\mathbb{R}^m} &= \langle y_{\partial,\mathrm{pl}}, \, \mathcal{W}^* \boldsymbol{y}_{\mathrm{rod}} \rangle_{L^2(\Gamma_{\mathrm{int}})}, \\
\mathcal{W}^* y_{\mathrm{rod}} &= v_G + \omega_G \, (y - L_y/2) \, .
\end{aligned}
$$

Results

Load $$f = \begin{cases} 10^5 \left[y + 10\,(y - L_y/2)^2\right] [\mathrm{Pa}], & \forall\, t < 2\,[\mathrm{ms}], \\ 0, & \forall\, t \geq 2\,[\mathrm{ms}], \end{cases} \qquad t_{\text{end}} = 10\,[\mathrm{ms}].$$

Play/Pause

Results

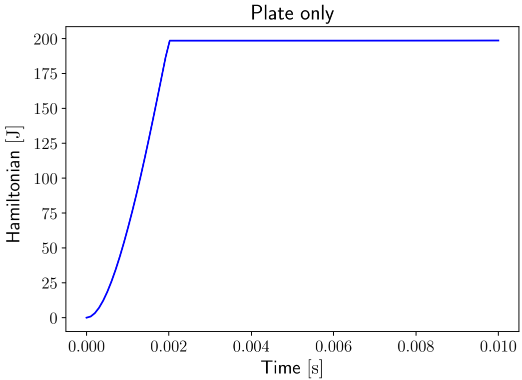
Plate only
Hamiltonian [J]
Time [s]
0
25
50
75
100
125
150
175
200
0.000
0.002
0.004
0.006
0.008
0.010

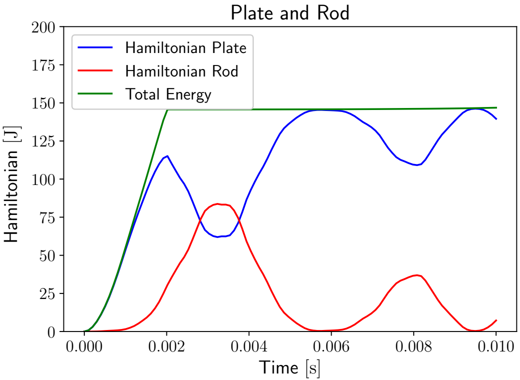
Plate and Rod
Hamiltonian Plate
Hamiltonian Rod
Total Energy
Hamiltonian [J]
Time [s]
0
25
50
75
100
125
150
175
200
0.000
0.002
0.004
0.006
0.008
0.010

Conclusion

Summarizing:

- Port-Hamiltonian formulation of floating bodies;
- Finite element discretization;
- Interconnection of subcomponents;
- Linearized case.

Some open questions:

- Stability and convergence of finite element;
- Time discretization;
- Non-linear model reduction of pHDAE;
- Control strategies.

Additional information[8]

[8] A. Brugnoli, V. Alazard D.and Pommier-Budinger, and D. Matignon. "Port-Hamiltonian flexible multibody dynamics". In: *Multibody System Dynamics* (2020). ISSN: 1573-272X. DOI: 10.1007/s11044-020-09758-6. URL: https://doi.org/10.1007/s11044-020-09758-6.

Thanks for your attention
Questions?

References I

O.P. Agrawal and A.A. Shabana. “Application of deformable-body mean axis to flexible multibody system dynamics”. In: *Computer Methods in Applied Mechanics and Engineering* 56.2 (1986), pp. 217–245.

A. Brugnoli, V. Alazard D.and Pommier-Budinger, and D. Matignon. “Port-Hamiltonian flexible multibody dynamics”. In: *Multibody System Dynamics* (2020). ISSN: 1573-272X. DOI: 10.1007/s11044-020-09758-6. URL: https://doi.org/10.1007/s11044-020-09758-6.

H. Egger et al. “On Structure-Preserving Model Reduction for Damped Wave Propagation in Transport Networks”. In: *SIAM Journal on Scientific Computing* 40.1 (2018), A331–A365. DOI: 10.1137/17M1125303.

D. De Klerk, D. J. Rixen, and S. N. Voormeeren. “General Framework for Dynamic Substructuring: History, Review and Classification of Techniques”. In: *AIAA Journal* 46.5 (2008), pp. 1169–1181. DOI: 10.2514/1.33274. URL: https://doi.org/10.2514/1.33274.

A. Macchelli, C. Melchiorri, and S. Stramigioli. “Port-Based Modeling and Simulation of Mechanical Systems With Rigid and Flexible Links”. In: *IEEE Transactions on Robotics* 25.5 (2009), pp. 1016–1029. DOI: 10.1109/TRO.2009.2026504.

A. Macchelli, C. Melchiorri, and S. Stramigioli. “Port-Based Modeling of a Flexible Link”. In: *IEEE Transactions on Robotics* 23 (2007), pp. 650 –660. DOI: 10.1109/TRO.2007.898990.

Volker Mehrmann and Riccardo Morandin. "Structure-preserving discretization for port-Hamiltonian descriptor systems". In: *Proceedings of the 59th IEEE Conference on Decision and Control*. 2019, pp. 6663 –6868.

Bernd Simeon. *Computational flexible multibody dynamics*. Springer, 2013.

Tamer M. Wasfy and Ahmed K. Noor. "Computational strategies for flexible multibody systems". In: *Applied Mechanics Reviews* 56.6 (Nov. 2003), pp. 553–613. ISSN: 0003-6900. DOI: 10.1115/1.1590354.

Institut Supérieur de l'Aéronautique et de l'Espace

10 avenue Édouard Belin – BP 54032

31055 Toulouse Cedex 4 – France

Phone: +33 5 61 33 80 80

www.isae-supaero.fr